

# A numerical model for the dissociative collision of the galaxy cluster Abell 2034

M. T. Moura<sup>1,2</sup> & R. E. G. Machado<sup>2</sup>

<sup>1</sup> Instituto de Física, Universidade Federal do Rio Grande do Sul, Porto Alegre, RS, Brazil, e-mail: micheli.moura@ufrgs.br

<sup>2</sup> Universidade Tecnológica Federal do Paraná, Rua Sete de Setembro 3165, Curitiba, Brazil.

**Abstract.** Galaxy cluster mergers are predicted by the hierarchical model of structure formation. Depending on collision parameters, the gas can separate from the dark matter in these clusters, configuring a dissociative collision. Abell 2034 is a galaxy cluster with  $\sim 720$  kpc of offset between the X-ray peak and the dark matter peaks, observed by gravitational lensings. From exploration of the parameters space using  $N$ -body hydrodynamic numerical simulations, we present a scenario for A2034 dissociative collision. In our proposed model, the collision occurs close to the plane of the sky, about 0.26 Gyr after the central passage, and with a small impact parameter. The numerical results agree with the observational results in terms of gas morphology at the appropriate separation distance between the substructures, preserving observational constraints such as, a discontinuity of the shock front near the northern substructure and temperature in the range of 10–12 keV. Also the model reproduces the displacement of the X-ray emission peak around 280 kpc to the dark matter halo of the southern substructure, and estimated time of the collision.

**Resumo.** Colisões entre aglomerados de galáxias são previstas pelo modelo hierárquico de formação de estruturas. Dependendo dos parâmetros da colisão, o gás pode se separar da matéria escura nesses aglomerados, configurando uma colisão dissociativa. O aglomerado de galáxias Abell 2034 apresenta  $\sim 720$  kpc de deslocamento entre o pico de emissão de raios-X e os picos de matéria escura, observados por lentes gravitacionais. A partir da exploração do espaço de parâmetros utilizando simulações numéricas hidrodinâmicas de  $N$ -corpos, apresentamos um cenário para a colisão dissociativa do A2034. Em nosso modelo proposto a colisão ocorre próxima ao plano do céu, cerca de 0.26 Gyr após a passagem central e com pequeno parâmetro de impacto. Os resultados numéricos concordam com os resultados observacionais em termos da morfologia do gás na distância de separação apropriada entre as subestruturas, preservando características observacionais como uma descontinuidade da frente de choque próxima à subestrutura norte e uma temperatura na faixa de 10–12 keV. Este modelo também reproduz o deslocamento do pico de emissão em raios-X por volta de 280 kpc até o halo de matéria escura da subestrutura sul, e tempo estimado da colisão.

**Keywords.** Galaxies: clusters: individual: A2034 — Galaxies: clusters: intracluster medium — Methods: numerical.

## 1. Introduction

Abell 2034 (A2034) is a galaxy cluster at  $z = 0.114$  in an post-collisional setting. A2034 has two substructures and has been widely observed by X-ray telescopes, showing a disturbed X-ray morphology with emission peak displaced in relation to the dark matter (DM) peaks. The substructures have mass ratio of 1:2.2 where both are separated by  $\sim 720$  kpc (Monteiro-Oliveira, et al. 2018). These results obtained from analysis of gravitational lensing and X-ray observations indicated a dissociative configuration. Dissociative collisions provide an extreme environment of interaction between galaxy clusters, where the dynamical properties of dark matter in relation to baryonic matter become evident. We aim to reproduce the dynamic history of the dissociative collision of Abell 2034 by numerical simulation. The procedure adopted and the results obtained will be described in section 2 and 3, respectively followed by summary.

## 2. Simulation setup

The method consists on carrying  $N$ -body hydrodynamic numerical simulations with parameters motivated by observations to simulate this specific merger context. We start by setting up two spherical galaxy clusters composed by gas and dark matter particles. This system will be evolved over time under specified conditions, as the parameters shown in Table 1. The code employed and details about the simulation are as follow:

- We adopt the GADGET-2 (Springel 2005) code which uses smoothed particle hydrodynamic (SPH);

- The initial conditions are composed of  $10^6$  gas particles and  $10^6$  DM particles for both substructures. The initial  $M_{200}$  conditions have 85% of dark matter mass and 15% of gas mass;
- The south and north substructures were created with masses similar to the virial masses:  $M_{200}^S = 2.35 \times 10^{14} M_{\odot}$  and  $M_{200}^N = 1.08 \times 10^{14} M_{\odot}$ . Galaxies, star formation, supernova and AGN feedback as well cosmological expansion are not considered.

We assume a Hernquist (1990) profile for DM halo density, and a Dehnen (1993) profile for gas density distribution, respectively:

$$\rho_h(r) = \frac{M_{\text{dm}}}{2\pi} \frac{a_{\text{dm}}}{(r + a_{\text{dm}})^3}, \text{ and } \rho_g(r) = \frac{3M_{\text{gas}}}{4\pi} \frac{a_{\text{gas}}}{(r + a_{\text{gas}})^4}, \quad (1)$$

where  $M_{\text{dm}}$  and  $M_{\text{gas}}$  represent total DM and gas mass, and consequently  $a_{\text{dm}}$  and  $a_{\text{gas}}$  is the scale length for DM and gas. Based on X-ray and lensing observations data, we explore the range of parameters that best agrees with the merger configuration. The parameters explored and the proper combination are described in Table 1.

## 3. Results

The main properties observed were reproduced by the numerical model proposed, such as temperature, collision close to the plane of the sky with small impact parameter, X-ray morphology, and the dissociative configuration with the proper distances between gas and DM.

**TABLE 1.** A sample of the exploration of collision parameters space. The columns indicates the parameter that is varied: impact parameter, initial velocity and inclination in relation to the plane of the sky. The bold values indicates the parameters of the best simulated model.

$b$ (kpc)	$v_0$ (km/s)	$i$ ( $^\circ$ )
<b>0</b>	<b>2000</b>	<b>0</b>
150	2000	0
250	2000	0
0	1500	0
<b>0</b>	<b>2000</b>	<b>0</b>
0	2500	0
<b>0</b>	<b>2000</b>	<b>0</b>
0	2000	13
0	2000	27
0	2000	41

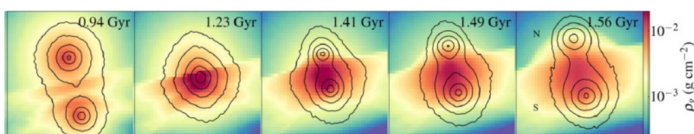


**FIGURE 1.** Time evolution of the substructures by gas density. At  $t = 1.49$  Gyr, the simulation correspond to 0.26 Gyr after the central passage. The contours lines represent the total projected mass in all frames. The ‘N’ and ‘S’ indicate the orientation of substructures at end of simulation.

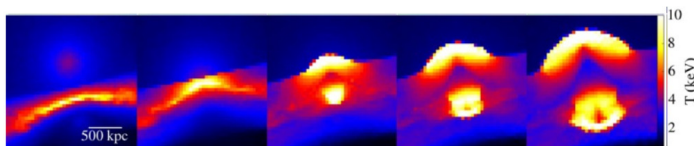


**FIGURE 2.** Time evolution of the substructures by emission-weighted temperature. The best moment of simulation is shown in the fourth panel.

The dynamics of the best model can be interpreted by looking at Fig. 1 and 2. We can see at Fig. 1 the gas density evolution in all frames for both substructures. We note in the first frame two structures approaching, where the cluster in the north at this moment is more massive than the cluster that is in the south. As the clusters get closer, shock fronts form, as illustrated in Fig. 2, and the density increases in the more central regions of the clusters. The clusters setting after the central passage changes, where the most massive cluster is now in the south and the least massive cluster is in the north. At 1.49 Gyr the gas morphology, and the appropriate temperature are reached, as well as the proper configuration of the substructures.

To find the parameters that would compose the best model presented, we did an exploration of the parameters space of simulation, searching for the best combination of velocity, impact parameter, inclination and X-ray gas morphology at the properly separation between the both dark matter halos.

Fig. 3 illustrates a small range of initial velocities explored to compose the best model described at Fig. 1 and 2. The gas temperature range is different for each velocity, as we can see from the shock fronts for the three frames. Knowing the observed temperature range expected for the shock fronts from Owers, et al. (2014), we found that the velocity range that produces the properly temperature is around 1500–2000 km/s.

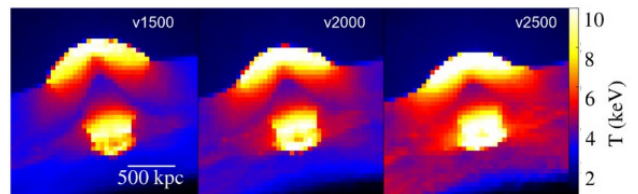


**FIGURE 3.** Initial velocity range for A2034 collision. The colors represents the temperature range for different velocities.

This approach of using the observed parameters from the literature to delimit the simulation parameters space exploration was used for the other constraints, i.e: impact parameter, to reproduce the morphology, and inclination to explore the range of possible inclination in relation to the plane of the sky. Besides these parameters, other aspects were reproduced by the best model of the simulation: time after the central passage ( $\sim 0.26$  Gyr) dissociation setting and temperature of the shock fronts with the properly observed position. Specifics details about the aspects simulated and mainly results can be found in Moura, et al. (2021).

#### 4. Summary

In summary, our proposed model to describe the dissociative collision of the galaxy cluster Abell 2034 consists of a frontal collision between both substructures: A2034S and A2034N. In our model, the northern cluster collides with the southern cluster with a small impact parameter and close to plane of the sky. The parameters adopted to compose the best model were: initial velocity = 2000 km/s, impact parameter = 0 kpc, inclination =  $0^\circ$  and scale lengths:  $a_g = a_h = 300$  kpc for A2034N and  $a_g = a_h = 400$  kpc for A2034S. From this model, the system is being observed at 0.26 Gyr after the central passage, when the distance between the total masses peaks reaches 720 kpc. We conclude that the presented numerical model satisfactorily reproduces the mains observational constraints of this specific merger collision.

*Acknowledgements.* UTFPR, SDumont – LNCC & Sociedade Astronômica Brasileira (SAB).

#### References

- Dehnen W., 1993, MNRAS, 265, 250
- Hernquist L., 1990, ApJ, 356, 359
- Kempner J. C., Sarazin C. L., Markevitch M., 2003, ApJ, 593, 291
- Monteiro-Oliveira R., Cypriano E. S., Vitorelli A. Z., Ribeiro A. L. B., Sodré L., Dupke R., Mendes de Oliveira C., 2018, MNRAS, 481, 1097
- Moura T. M., 2021, MNRAS, 500, 1858
- Owers M. S., et al., 2014, ApJ, 780, 163
- Springel V., 2005, MNRAS, 364, 1105